Communications Earth & Environment https://doi.org/10.1038/s43247-026-03233-4

Article in Press

Amazonian fog harbors viable microbes

Received: 23 July 2025

Accepted: 16 January 2026

Cite this article as: Godoi, R.H., Hara, E.L., Sebben, B.G. *et al.* Amazonian fog harbors viable microbes. *Commun Earth Environ* (2026). https://doi.org/10.1038/s43247-026-03233-4

Ricardo H. M. Godoi, Emerson L. Y. Hara, Bruna G. Sebben, Philip E. Taylor, Dulcilena M. Castro e Silva, Sebastian Brill, Valter B. Duo Filho, Glaucio Valdameri, Luciano F. Huergo, Rosaria R. Ferreira, Cléo Q. Dias-Junior, Maurício C. Mantoani, Fábio L. T. Gonçalves, Rachel I. Albrecht, Nurun N. Lata, Gregory Vandergrift, Swarup China, Carlos I. Yamamoto, Rodrigo F. C. Marques, Rodolfo D. Piazza, Rodrigo A. F. Souza, Theotonio Pauliquevis, Paulo Artaxo, Luiz A. T. Machado, Heitor Evangelista, Jéssica C. dos Santos-Silva, Sanja Potgieter-Vermaak, Subha S. Raj, Christopher Pöhlker, Jens Weber, Bettina Weber, Laudemir C. Varanda, Ivan Kourtchev, Scot T. Martin, Ulrich Pöschl & Meinrat O. Andreae

Amazonian fog harbors viable microbes

Ricardo H. M. Godoi[1*], Emerson L. Y. Hara[1], Bruna G. Sebben[1], Philip E. Taylor[2], Dulcilena M. Castro e Silva[3], Sebastian Brill[4], Valter B. Duo Filho[3], Glaucio Valdameri[5], Luciano F. Huergo[6], Rosaria R. Ferreira[7], Cléo Q. Dias-Junior[8], Maurício C. Mantoani[9], Fábio L. T. Gonçalves[9], Rachel I. Albrecht[9] , Nurun N. Lata[10], Gregory Vandergrift[10], Swarup China[10], Carlos I. Yamamoto[11], Rodrigo F. C. Marques[12], Rodolfo D. Piazza[12], Rodrigo A. F. Souza[13], Theotonio Pauliquevis[14], Paulo Artaxo[15], Luiz A. T. Machado[4,15], Heitor Evangelista[16], Jéssica C. Santos-Silva[1], Sanja Potgieter-Vermaak[17], Subha S. Raj[4], Christopher Pöhlker[4], Jens Weber[4], Bettina Weber[4,18], Laudemir C. Varanda[19], Ivan Kourtchev[20], Scot T. Martin[21], Ulrich Pöschl[4], Meinrat O. Andreae[4,22]

1. Environmental Engineering Department, Federal University of Paraná-PR, Curitiba, Brazil;
2. Department of Rural and Clinical Sciences, La Trobe Rural Health School, La Trobe University, Melbourne, Australia;
3. Parasitology and Mycology Center, Department of Environmental Mycology, Lutz Institute, São Paulo, Brazil;
4. Multiphase Chemistry and Biogeochemistry Departments, Max Planck Institute for Chemistry, Mainz, Germany;
5. Graduate Program in Pharmaceutical Sciences, Laboratory of Cancer Drug Resistance, Federal University of Paraná -PR, Curitiba, Brazil;
6. Sector litoral- Matinhos, Federal University of Paraná-PR, Matinhos, Brazil;
7. Amazon Tall Tower Observatory (ATTO), Program Large Scale Biosphere-Atmosphere in the Amazon-AM, Manaus, Brazil;
8. Physics Department, Federal Institute of Pará, Pará, Brazil;
9. Department of Atmospheric Sciences, Institute of Astronomy, Geophysics, and Atmospheric Sciences, University of São Paulo, São Paulo, Brazil;
10. William R. Wiley Environmental and Molecular Sciences Laboratory, Pacific Northwest National Laboratory, Richland, United States of America;
11. Department of Chemical Engineering, Federal University of Paraná-PR, Curitiba, Brazil;
12. Chemistry Institute, São Paulo State University-SP, São Paulo, Brazil;
13. Meteorology Department, State University of Amazonas-AM, Manaus, Brazil;
14. Department of Environmental Sciences, Federal University of São Paulo-SP, Diadema, Brazil;
15. Physics Institute, University of São Paulo-SP, São Paulo, Brazil;
16. LARAMG, Rio de Janeiro State University-RJ, Rio de Janeiro, Brazil;
17. Department of Natural Sciences, Manchester Metropolitan University, Manchester, United Kingdom;
18. Institute for Biology, Division of Plant Sciences, University of Graz, Graz ,Austria;

19. Physical-Chemistry Department, Chemistry Institute of São Carlos, University of São Paulo, São Carlos, Brazil;
20. Centre for Agroecology Water and Resilience, Coventry University, Coventry, United Kingdom;
21. School of Engineering and Applied Sciences and Department of Earth and Planetary Sciences, Harvard University, Cambridge, United States of America;
22. Department of Geology and Geophysics, King Saud University, Riyadh, Saudi Arabia.

*e-mail: rhmgodoi@ufpr.br

ABSTRACT

Fog formation over tropical forests remains poorly characterized, despite its potential role in bioaerosol dispersion and ecosystem processes. Here, we analyzed fog samples collected at the Amazon Tall Tower Observatory using flow cytometry and culture-based techniques to characterize viable microbial communities. Microbial cell concentrations varied over an order of magnitude across 13 fog events, reaching up to 8×10^4 cells per ml of fog water. Flow cytometry consistently detected metabolically active cells, while culturing and mass spectrometry-based identification yielded eight viable bacterial species and seven fungal taxa. The bacteria *Serratia marcescens*, *Ralstonia pickettii* and *Sphingomonas paucimobilis* exhibited seasonal variations in prevalence. The fungal species identified were primarily mesophilic saprophytes and endophytes, commonly associated with soil and plant surfaces. Our findings indicate that fog harbors viable microbes, including *Serratia marcescens* and *Ralstonia pickettii*, which may imply a relevance of fog for microbial dispersal, colonization and nutrient cycling in the Amazon rainforest.

Keywords: Fog microbiome; Bioaerosol transport; Amazon rainforest; Microbial deposition; Tropical bioaerosols; Climate change impacts

Introduction

The Amazon rainforest, harboring over 10% of global biodiversity and 150–200 Pg C [1-3], sustains Earth's climate[4-6], acting as a "water pump". Through evapotranspiration, it generates up to 50% of regional rainfall, sustaining moisture-dependent biomes and economic activities across South

America[7]. Its hydrological contribution is often studied through rainfall, yet, fog clouds, another relevant component, remain unexplored. In other ecosystems, fog may act as a medium for microbial persistence [14], prompting the question of how such processes may unfold in the Amazon. However, climate-driven disturbances, including warming temperatures and altered precipitation patterns, threaten large-scale forest loss, potentially disrupting hydrological cycles and amplifying global warming through carbon emissions and feedback mechanisms[5,8]. These changes could impact fog formation, and, furthermore, decrease the microbial dispersal and nutrient cycling in the forest canopy promoted by those clouds, though this requires further investigation. Previous studies, such as Pöhlker et al. (2018) and Prass et al. (2021), have characterized bioaerosols and clouds in the Amazon. This study is the first to investigate viable microbial communities in Amazonian fog droplets. We used flow cytometry and Matrix-Assisted Laser Desorption/Ionization Time-of-Flight Mass Spectrometry (MALDI-TOF MS) to assess viability and taxonomic diversity, focusing on seasonal dynamics and fog's ecological role.

The exchange of water, gases, and particles between the biosphere and the atmosphere is highly dynamic[9]. Rising patches of fog from the forest canopy are a characteristic feature of the Amazon's intense hydrological cycle. Fog is a low-altitude cloud, driven by the physics described for convective clouds[10]. Water vapor supersaturation (S) activates a fraction of atmospheric aerosol particles into fog droplets.

Fog formation involves water vapor supersaturation, where aerosol particles act as Fog Condensation Nuclei (FCN). The Köhler theory, combining the Kelvin effect (increased vapor pressure over curved surfaces) and solute effects, determines activation thresholds, with microbial surfaces potentially lowering energy barriers via hygroscopic properties[11]. This process is mutually facilitative, whereby microorganisms may promote droplet nucleation because they stand to gain from being in water: (i) droplets provide a protective environment, shielding microorganisms from dehydration, UV radiation, and pollutants, potentially extending their viability for long-distance transport and colonization; and (ii) microorganisms may serve as nucleation surfaces, potentially enhancing droplet formation. Electrostatic interactions, influenced by the negative surface charge of both droplets and microbial cell walls (e.g., lipopolysaccharides in Gram-negative bacteria), may further facilitate microbial entrainment. These interactions, coupled with seasonal variability in aerosol and

microbial abundance, suggest a potential role for fog in microbial dispersal and ecosystem functioning in the Amazon rainforest. Particle size, chemical composition, and hygroscopicity determine which aerosol fraction acts as Cloud Condensation Nuclei (CCN)[12] or FCN[13], the particles that initiate droplet formation in clouds and fog, respectively. Low-altitude supersaturation (S) can result from radiation cooling, advection cooling, the mixing of warm and cold air masses, or frontal passages[14]. In the Amazon, nighttime radiative cooling is the primary driver of fog formation, reaching its maximum just before sunrise. Post-rainfall colder downdrafts interacting with the warm and moist canopy initiate the characteristic fog plumes observed above the forest[15].

The S levels in fog are typically below 0.1%[16,17], lower than S at the base of convective clouds, which ranges between 0.1 and 1%[18]. Under these low S conditions, larger aerosol particles (diameters 300–500 nm) activate preferentially as FCN[19]. This activation depends on the hygroscopicity parameter κ (typically ranging from 0.1 to 0.4), which characterizes the ability of aerosol particles to uptake water and consequently influences their effectiveness as FCN[20]. Chamber studies conducted at low supersaturation have demonstrated that the chemical composition of FCN plays a crucial role in droplet activation efficiency and stability. For instance, uncoated graphite particles exhibited markedly lower activation compared to more hygroscopic or coated particles, underscoring the influence of FCN surface properties and chemistry on fog microphysics and droplet formation dynamics[21]. Biological aerosols, acting as FCN, facilitate microbial dispersal in fog, with seasonal variability driven by local and transported particles[22,23].

The total aerosol particle concentration in the Amazon region exhibits significant seasonal variability, ranging from a few hundred particles per cubic centimeter during pristine periods in the wet season to tens of thousands per cubic centimeter under heavy biomass-burning conditions in the dry season[24]. Specifically, aerosol number concentrations for particles larger than 300 nm—those most relevant to fog droplet formation—typically range from about 5 to 60 cm^{-3} in the Amazon[25].

Likewise, the exchange of primary biological aerosol particles (PBAPs) between the forest ecosystem and the atmosphere is dynamic. These PBAPs comprise a wide diversity of fungal, fern, and bryophyte spores, bacteria and pollen, as well as amorphous debris and emission-associated liquids[26-28]. The atmospheric life cycle of PBAPs in the Amazon, with its exuberant biodiversity, still

poses numerous open questions. Especially interesting and largely unstudied is the interaction of PBAPs with cloud or fog droplets.

When microbes become trapped in cloud or fog droplets, they initiate several key processes: (i) metabolic activities, including spore germination and the release of cytosolic materials[12]; (ii) aqueous phase chemistry, such as changes in oxidation capacity, amino acid distribution, and decomposition of organic matter[29]; and (iii) alterations to the aerodynamic properties of the droplets[30]. These processes have significant ecological implications: (iv) the droplets provide shelter against dehydration, UV radiation, and pollutant exposure[31], which can (v) extend the atmospheric lifetime of microorganisms, facilitating their long-distance dispersal and colonization of new habitats[32]. Additionally, the modified aerodynamic properties influence the timing and location of microbial deposition, affecting when and where these organisms settle on surfaces[30].

In this study, we investigate the abundance and viability of microorganisms in fog droplets at the Amazon Tall Tower Observatory[33] by using high-resolution microbiological analyses, aerosol, and micrometeorological data. Here, we explore the mechanisms for microbial dispersal and transformation that fog plays in the biosphere-atmosphere coupling of the Amazon forest, which may also have potential roles in other fog-influenced ecosystems. This study highlights fog as a hitherto overlooked atmospheric pathway for microbial exchange, with potential implications for ecological processes in tropical forests.

Material and Methods

Fog Sampling

Fog samples were collected at the Amazon Tall Tower Observatory (ATTO) site[33]. It is located approximately 150 km northeast of Manaus, Brazil, in the Uatumã Sustainable Development Reserve (02°08'45.13"S, 59°00'20.12"W), 130 m above mean sea level[33]. The site is equipped with several research towers for access to the atmosphere at different heights, as well as a wide range of ground-based instruments for measuring atmospheric properties and other environmental parameters [33]. The height of the main tower is 325 m. The area is covered by dense primary Terra

Firme forest with an average canopy height of about 30 to 37 m and emergent trees reaching 45 to 50 m. The predominant climate is tropical humid. It is characterized by a pronounced wet season from February to April and a dry season from August to October. The other months are considered as a transition between seasons[33].

A Caltech Active Strand Cloud Collector (CASCC), specifically the smaller CASCC2 model, was used to collect fog (Fig. S1). The sterile sampler was installed at a height of 43 m on a small platform on the north-eastern side, which is the main wind direction at ATTO during most times of the year. The sampling device was rigorously decontaminated by rinsing with Milli-Q ultrapure water, followed by ultraviolet (UV) sterilization for 30 min under controlled laboratory conditions. The sterile CASCC2 was sealed in polyethylene film and transported to the ATTO site to prevent environmental contamination. The CASCC2 sampler operated at a flow rate of 24.5 m^3 min^{-1}. The CASCC2 is a non-size-fractionating collector that impacts fog droplets above a minimum size threshold (~5–10 µm), capturing the majority of the fog water content and associated microbial content, but providing no size resolution of the residual fog condensation nuclei. The device was thoroughly rinsed with Milli-Q ultrapure water to minimize the risk of cross-contamination between sampling events. Following decontamination, it was stored in a weather-protected, contamination-free environment until the next sampling event. Six rows of Teflon wires were employed to impact the fog droplets, and UV-sterilized polyethylene bottles were used to collect the fog water (Fig. S2)[34]. Control rinses were performed by collecting and analyzing water samples for microbial presence using flow cytometry to ensure that the Milli-Q water used for cleaning was free of microbial contamination. No microbial cells were detected in any of the control samples, thereby confirming the sterility of the cleaning procedure and minimizing concerns about potential cross-contamination. To preserve sample integrity, sampled fog water was stored in 125 ml polyethylene bottles that had been previously washed with Triton detergent, then sterilized by subjecting them to sonication in ultrapure water for 30 min, followed by UV sterilization under a laminar flow hood for 15 min. After sampling, the bottles were maintained under refrigeration at -2°C until further analysis, which was conducted within two weeks. Table S1 summarizes four key measures implemented to control contamination: equipment decontamination, sterilization of collection materials, sterility validation, and sample storage and analysis.

Fog sampling was conducted every night throughout the study period. The equipment was operated on a timer to maintain consistent sampling intervals. This overnight sampling strategy was based on diel trends observed with the fog monitor installed at the ATTO tower (see the Results and Discussion section). Three sampling campaigns were conducted (Table 1): (1) 24 April–9 May 2022, late wet season (6 samples); (2) 7–23 October 2022, late dry season (4 samples); and (3) 10–25 January 2023, early wet season (3 samples). In total, 13 fog samples with collected liquid water were obtained. Each campaign lasted for 15 to 20 days. Samples collected during active rainfall ($P \geq 0.5$ mm/h) were discarded to prevent significant dilution or contamination; however, samples with minimal precipitation ($P < 0.5$ mm/h), such as S3, were retained if fog conditions persisted and dominated the sampling period.

Meteorology, fog time series, and fog profiles

The occurrence of water (super)saturation was analyzed with profiles of micrometeorological data, measured on the 81 m tower (for details see Andreae et al., 2015), which is 400 m away from the fog sampler on the tall tower. One indication for the presence of fog was a relative humidity exceeding 95%. An independent indication was provided through a measurement of atmospheric visibility, which was conducted continuously with an optical fog sensor ONED 250 (Eigenbrodt GmbH & Co. KG, 21255 Königsmoor, Germany). The instrument was installed at 43 m at the same level as the CASCC2, and data were recorded at an interval of 1 min. Fog events—defined as instances of visibility below 1000 m—were recorded multiple times per minute between September 2014 and December 2018. This threshold aligns with the international standards established by the World Meteorological Organization (WMO) and the American Meteorological Society (AMS). The monthly frequency of these events, presented in Fig. S3, was used to identify periods of high fog incidence and temporal variability, ensuring that sampling efforts captured the most representative conditions. Figure S3 is based on data from 2014-2018 to establish historical patterns of fog occurrence, using the optical fog sensor ONED 250, while the visibility data up to 2023, shown in Figure 1, complement the seasonal and diurnal analyses of the 2022-2023 campaigns.

The continuous visibility data is available for Campaign 2. For Campaign 1, however, no data were available due to technical issues with the sensor. To address the absence of visibility data for

Campaign 1 due to technical issues with the sensor, relative humidity exceeding 95% was used as a robust proxy for fog events, consistent with established meteorological criteria, ensuring comparability with Campaigns 2 and 3. Relative humidity time series for all campaigns are shown in Supplementary Fig. S4. During Campaign 3, the continuous visibility measurement at 43 m was interrupted, and the sensor was installed on the custom-built automatic Robotic Lift (RoLi) system[34]. The RoLi system was installed at the southern corner of the 325-m ATTO. During Campaign 3, 48 high-resolution vertical profiles per day of meteorological data, as well as visibility, were measured between 8 and 318 m. At the vertical speed of 0.3 m s^{-1}, one full profile took around 15 minutes. For measurement of meteorological parameters, the WS500-UMB Smart Weather Sensor (OTT HydroMet Fellbach GmbH, 70736 Fellbach Germany) was used. The detection intervals were 1 min^{-1} for temperature and relative humidity and 1 Hz for air pressure, wind speed, and wind direction. Data gaps, when present, were caused by maintenance or by strong winds, leading the software security mechanism to prevent operation of the RoLi. Visibility data were used for a statistical analysis of fog event occurrences.

Flow Cytometric Analysis and Zeta potential

The flow cytometric analysis was performed using a BD FACS Celesta (Becton Dickinson) Flow Cytometer, following a standard protocol[35]. The fog water samples were vortexed for 30 s and 500 µL aliquots were transferred to 5 mL flow cytometry tubes. The fluorescent dyes Rhodamine 123 (Sigma-Aldrich) at 10.0 µmol L^{-1} and Hoechst 33342 (Invitrogen) at 3.0 µmol L^{-1} were added to half the samples (dyed samples). Staining with both dyes followed international standard protocols routinely applied in flow cytometry for the assessment of microbial viability in environmental samples (membrane potential via Rhodamine 123 and total DNA staining via Hoechst 33342, and equivalent established procedures for Rhodamine 123 as used in numerous atmospheric microbiology studies). The other half of the samples were incubated without the addition of dye (control samples), and ultrapure water was used as a blank. The dyed samples, control samples, and blanks were

incubated for 15 min before analysis on the flow cytometer. Data were acquired for 60 s at 60 µL min^{-1} flow rate. The analysis was performed using the 450/50 nm channel for Hoechst-33342 (excitation at 355 nm) and the 530/30 nm channel for Rhodamine-123 (excitation at 488 nm). Zeta potential and hydrodynamic diameter were measured in a Zetasizer ZSNano (Malvern Instruments). The samples were analyzed upon receipt and measured in triplicate to ensure reproducibility.

Microorganism Cultivation, Isolation, and Classification using MALDI-TOF-MS

Fog water samples were homogenized, and 2 ml aliquots were centrifuged at 18,000 rpm for 2 min. Subsequently, a 10.0 µL aliquot was seeded in a Petri dish containing DRBC (Dichloran Rose Bengal Chloramphenicol agar) for fungal culture, and a tryptic soybean broth (TSB, Soybean Agar) to cultivate bacteria[36]. As per Mantoani et al., bacterial and fungal plates were incubated at 35°C for 48 h and at 30°C for 7 days, respectively, and were then processed at the Mycology Laboratory at the Adolfo Lutz Institute in São Paulo for isolation and identification[37]. After cultivation, bacterial and fungal species were classified at the species level, using MALDI-TOF MS (Bruker Daltonics, Billerica, Massachusetts, USA)[38]. As described in Mantoani et al. 2023, based on the time of flight of laser-excited ribosomal proteins in a lipid matrix, this technology can interpret specific spectral masses of different microorganisms[38]. Calibration is performed using a standard strain of *E. coli* 16S that contains known spectra, ensuring the sensitivity of the test and identification. Through the results provided in the score registered at the instrument, genus (scores between 1.7 and 1.9) and species (scores above 2.0) are identified[38,39].

Analysis of Data

Given that the data did not meet the normality and homoscedasticity assumptions and the sample sizes varied across seasons, the difference in cell counts obtained from flow cytometry were assessed using the Kruskal-Wallis test, a non-parametric method. This examination was conducted at a significance level of $\alpha = 0.05$, utilizing Statistica software version 14.0.0.15 (Statistica, 2022). The proportions of bacteria and fungi were determined descriptively by calculating the frequency of occurrence of each species relative to the total sample size.

Results and Discussion

Physical characteristics and temporal dynamics of fog events

Over a 30-year period, data collected by the National Institute for Space Research (INPE) indicate that the average monthly precipitation ranges from 260 to 330 mm and the average temperature from 23 to 32 °C during the rainy months of April and May, coinciding with our fog collection in campaign 1. In contrast, in October, which marks the late dry season and aligns with campaign 2, the average monthly rainfall drops below 130 mm, and temperatures fluctuate between 23 and 34 °C. In January, a transitional period between dry and wet seasons corresponding to campaign 3, average monthly precipitation is approximately 280 mm with temperatures spanning from 23 to 31 °C. The meteorological conditions observed during the three fog sampling campaigns are summarized in Table S2 and align with the established climatic averages for the respective seasons, indicating that the sampling conditions were representative of typical seasonal patterns.

Meteorological and related parameters, such as humidity, cloud cover, nocturnal radiative cooling, suspended particulate matter (SPM), as well as rainfall intensity and frequency affect the formation of fog. Fog occurrence was more frequent in the wet than in the late dry season (Fig. 2). While being predominant during the wet season, fog events also occurred during the early wet season and the late dry season, albeit with lower frequency and shorter duration.

The diel trends in fog occurrence are shown in Fig. 1. Fog formation is typically most pronounced during late night and early morning hours, especially between 03:00 and 07:00 local time (LT). The fog builds up gradually during the second half of the night and dissipates rather suddenly around 07:00 LT with the onset of convective mixing and the development of the convective boundary layer. A secondary and weaker fog peak occurred in the late afternoon, typically after convective rain showers. The diel trends in Fig. 1 are similar across all months, with a minimum visibility around 3:00 to 4:00 LT. The late wet season months March, April and May had the lowest visibility and most pronounced diel patterns, whereas the late dry season months July, August, and September are associated with the lowest visibility amplitude.

The three fog sampling campaigns covered 46 nights and 13 fog events that were observed and sampled at ATTO. The fog events usually occurred between 03:00 and 07:00 LT, consistent with

Fig. 1. For campaigns 1 and 2, Fig. 3 shows time series of the entire aerosol size distribution, rainfall, relative humidity, and fog occurrence, in relation to the individual fog sampling periods. Most fog periods are associated with characteristic 'notches' in the contour plots of the aerosol size distributions, collocated with a decrease of visibility (Fig. 3B) and RH reaching saturation (Figs. 3A and B). Particularly clear examples are, for instance, the sampling periods S8 and S9 on 16th and 18th Oct 2022 in Fig. 3B. The depth of these notches indicates which aerosol particle sizes were activated as FCN. Figure 3B suggests that particles with diameters > 300 nm were prone to act as FCN, and therefore not visible anymore in the aerosol size spectra. Critical diameters in this range have also been reported in previous studies conducted in contrasting environments, such as semi-urban Paris[41], suggesting that similar activation thresholds can arise under different aerosol and thermodynamic conditions. The fog-related notches are less pronounced during the late wet season (Fig. 3A, Campaign 1) than during the late dry season (Fig. 3B, Campaign 2). This suggests a seasonal dependence of aerosol–fog interactions, driven by aerosol particle properties, water-vapor supersaturation, or both. With the data analyzed in this study, such potential seasonality cannot yet be quantified. Nevertheless, it can be concluded here qualitatively that the occurrence and "depth" of the fog-related notches appear highly variable and are likely governed by seasonal differences in FCN and microbial composition and supersaturation (Artaxo et al., 2013; Pöhlker et al., 2018; Souza et al., 2021, Barbosa et al., 2022). We hypothesize that variations in supersaturation play the primary role, which remains to be verified in future studies. Additionally, differences in FCN composition – particularly near the critical diameter for activation into fog droplets – may also exert a measurable influence (Dusek et al., 2006; Pöhlker et al., 2021). In addition to the aerosol-fog interaction, the more frequent precipitation and the associated rain-related scavenging, causes similar patterns in the aerosol size spectra and therefore partly masks the fog-related notches.

During the fog sampling campaign 3, the operation of the Robotic Lift (RoLi) system[34] with a meteorological and aerosol instrument package, together with the visibility sensor, allowed analysis of the vertical profiles of the morning fog layers. As a characteristic example and corresponding to one individual sampling period, Fig. 4 illustrates the diel cycle of vertical profiles for selected meteorological parameters and aerosol number concentration between 300 nm and 10 µm between 14 January and 16 January 2023, covering the fog event S11 on 15 January 2023. The visibility in

Fig. 4E represents the nighttime build-up of the fog layer with a minimum around 400 m at 04:00 LT on 15 January 2023. The fog layer was most pronounced between the canopy top, around 30 m, and about 150 m. Fog in this height range has been observed frequently, indicating that the fog sampling height of 43 m was well chosen. In the case shown in Fig. 4, fog was present at the sampling height for most of the night, until approximately 06:00 LT on 15 January 2023. On 14 January 2023, another fog event was observed after midnight, lasting until around 08:00 LT. The rise of the fog layer driven by the formation of the convective boundary layer can be clearly seen in Fig. 4E. During the sampled fog event S11 on 15 January 2023, the aerosol number concentration inside the fog layer was significantly reduced from ~ 5 cm^{-3} before to ~0.5 cm^{-3}, clearly showing that a large fraction of aerosol particles greater than 300 nanometer were activated into fog droplets. The occurrence of these “fog holes” is frequently observed in vertical profiles of aerosol number concentration during fog events, highlighting the importance of larger aerosol particles e.g. fungal spore, in the formation of fog droplets.

Microbial abundance and viability in Amazonian fog droplets

Although our sampling was limited to 13 fog events, these were strategically collected during the late wet season, late dry, and early wet season, which are the primary periods of fog formation at the Amazon Tall Tower Observatory (ATTO), as fog occurrences are less frequent during the late dry season. The relatively small sample size reflects the logistical challenges of collecting fog water under controlled conditions in a remote rainforest environment. Flow cytometric analysis was applied to quantify the number concentration of microorganisms in the fog samples (Fig. 5). The lowest concentrations ranged around $6 \cdot x\ 10^4$ to $7 \cdot x\ 10^4$ cells per ml of fog water (e.g., samples S2 and S6), whereas the highest concentrations reached nearly 1×10^5 cells per ml of fog water (e.g., samples S1 and S7). Variation between individual samples, however, was remarkably large. In some cases, cell concentration of subsequent samples, as S1 and S2, dropped by about one order of magnitude (Fig. 5). This could be explained by a corresponding decrease in the aerosol particle concentration in the size range of large accumulation mode and coarse mode particles, which account for the majority of FCN. After S1, when very high cell numbers were counted, there were several rain events, which effectively removed particles from the atmosphere, and S2 (3,450 cells

ml-1) was taken 4 days later, shortly after a rain event (see Fig. 3). Also between S7 (98,466 cells ml^{-1}) and S8 (67,000 cells ml^{-1}), collected during the late dry season, major differences in cell numbers were assessed, and also here this decreased number in S8 could be caused by a previous rain event. Comparing samples S8 and S9 (17,200 cells ml^{-1}), however, the further decrease in cell number is not linked to a decrease in coarse aerosol particle concentrations. Here, meteorological conditions[42], including post-rainfall effects that initiate fog formation prior to sampling of S8, and fog event length[10] could potentially enhance microbial entrainment during sampling of S8. The high variability observed in cell counts is consistent with previous studies of Amazonian bioaerosol concentrations, which also report strong temporal fluctuations[42]. These studies suggest that meteorological conditions, aerosol size (>300 nm), relative humidity, and wind patterns may influence the abundance and entrainment of biological particles in fog droplets.

For additional comparison, data from Campaign 3 (early wet season, January 2023) obtained via the RoLi system show relatively small depletions in aerosol size distributions >300 nm, similar to those in Campaign 1, owing to predominantly wet conditions with precipitation of ~280 mm and low environmental loading of coarse aerosols (see Fig. S3 in the supplementary material for representative distributions). This consistency reinforces that meteorological variations and aerosol size (>300 nm) might primarily explain the observed variability, with secondary influence from seasonal microbial composition (e.g., greater saprophytic diversity during the wet season, associated with soils and plants).

Meteorological variables were analyzed during the fog collection periods, yielding weak correlations with cell concentration (Fig. S4b). Moderate correlations were found for temperature (R=0.30) and relative humidity (R=-0.42), considering the average data from 12 hours previous to each fog event (Fig. S4a). This indicates that the conditions preceding fog formation might influence the microbial community more than those during fog collection.

Similarly, the occurrence of dominant bacterial taxa, such as *Serratia marcescens* and *Ralstonia picketti*, was more frequent in wetter campaigns, potentially reflecting moisture-dependent growth and aerosolization from soil and plant surfaces, while fungal taxa (e.g., mesophilic saprophytes) showed broader presence across seasons, but with hints of wind-driven transport from prevailing wind directions (e.g., northeast in wet seasons; Fig. 5B). These patterns suggest that fog formation

under high-RH, low-temperature conditions may enhance microbial entrainment and viability in the Amazonian atmosphere.

Late wet, late dry, and early wet season comparisons did not show significant differences between the three sampling campaigns, with similar averages 15.186, 24,214, 13,729 cells per ml of fog water in the late wet, late dry, and early wet season, respectively. Also a Kruskal-Wallis test indicated no statistically significant difference between the average cell concentrations ($H\ 2,10) = 0.769$; $P = 0.49$). This suggested similarity between seasons is caused by the large variability between samples and the low number of samples per season. Thus, an increase in sample number could elucidate differences between seasons, which are currently disguised by the low sample number.

To assess whether fog events themselves may explain part of this variability, we examined the relationship between cell concentration peaks and periods of reduced visibility. Notably, peaks in cell counts, such as those observed in fog samples S7 and S8, coincided with periods of intensified fog formation. For instance, S7 exhibited a significant peak in cell count (98,000 cells per ml of fog water) during a period of low visibility and high particle number concentration. Similarly, S8, with a high cell count of 67,000 cells per ml of fog water, aligns with low visibility and increased particle number concentration. Even samples having lower cell counts, like S9 (17,000 cells per ml of fog water), still corresponded to reduced visibility periods, and S10 showed a significant number of cells (40,07700 cells per ml of fog water) during the fog event. This reduced visibility during S9 is evident in Fig. 3B. The period is also characterized by a depleted aerosol surface size distribution (dS/dlogD) in the 300 nm to 10 µm range. The variability in microbial cell concentrations, such as the notable differences between samples S7 (98,466 cells per ml of fog water) and S9 (17,200 cells per ml of fog water) during the late dry season, may extend beyond influences from coarse aerosol particle concentrations alone. Meteorological conditions, including post-rainfall effects that initiate fog formation, could enhance microbial entrainment in certain events, potentially elevating counts despite seasonal patterns[22]. High humidity (>95%) and negative zeta potentials (−12.3 to −27.5 mV) support the incorporation of viable microbes via electrostatic interactions, aligning with the negative charge of bacterial cell walls in Gram-negative taxa[30]. Additionally, wind patterns may

influence the abundance and entrainment of biological particles[42], complementing seasonal aerosol effects from biomass burning[25].

Zeta potential measurements of bulk fog samples yielded consistently negative values, which are compatible with the negative surface charges typical of Gram-negative bacterial cell walls, such as those in prevalent taxa like *Serratia marcescens* and *Ralstonia pickettii*. However, these measurements reflect the net charge of all dispersed species in the condensed fog water, including potential contributions from organic acids, dissolved ions, and abiotic particulates, rather than isolated microbial surfaces. Without sterile controls or single-particle analyses, direct attribution to microorganisms remains tentative. Nonetheless, the observed values are consistent with electrostatic interactions facilitating microbial incorporation into fog droplets, as hypothesized. Microorganisms may contribute to fog formation and persistence by acting as efficient condensation nuclei, particularly in low-supersaturation environments, as evidenced by chamber studies on biological particle activation and field observations of enhanced microbial viability in fog[41,30,43]. Given typical Amazon fog droplet densities of 10^7–10^8 m^{-3} and a liquid water content (LWC) of 0.1–0.5 g m^{-3}, microbes likely occupied 0.01–0.5% of droplets on average, with potential clustering in a subset of larger droplets.

The highest microbial concentrations observed in the present study (9.8×10^4 cells ml^{-1} fog water) are directly comparable to those reported in non-tropical cloud water (typically 2×10^4–1×10^5 cells ml^{-1} [43]) and fall within the range found in atmospheric aerosol studies[45], indicating no unusual enrichment in near-surface Amazonian fog.

Taxonomic identification and ecological relevance of culturable fog microorganisms

To complement the cytometric evidence of metabolically active viable cells in fog water — primarily determined by Rhodamine 123 staining of intact mitochondrial membrane potential, with Hoechst 33342 used as a counterstain for total intact microbial cells — we next investigated the identity and potential ecological roles of culturable microorganisms recovered from the same fog events. Ecological roles, such as nutrient cycling or decomposition, were inferred based on the known functions of identified taxa in other environments. As suggested for temperate regions[31,44], the most readily culturable microorganisms are likely to contribute to the phylloplane ecology of the

Amazon rainforest. This environment is particularly dynamic due to high humidity, abundant organic matter, and the exceptional diversity of microorganisms and plants. Fog droplets, acting as transient microhabitats, may facilitate the transfer of these culturable species across canopy layers, linking aerial microbial communities to surface colonization processes and potentially influencing phyllosphere diversity.

Across the three campaigns, eight viable bacterial species were detected in fog samples (Fig. 5). *Serratia marcescens* and *Ralstonia picketti* were the most frequently detected bacteria, appearing in 45% of the samples. Seven bacterial species were detected during the wet season, while only four were detected during the late dry season. *Serratia marcescens* and *Ralstonia pickettii*, both known to thrive in moist environments[46], were the dominant bacteria during the wet season, while *Sphingomonas paucimobilis*, which is known to be more resilient to dry conditions[47], was detected only at the late dry season. The bacterial species identified in fog water samples were detected more frequently during wet periods, which coincided with higher occurrences of fog and precipitation events (Fig. 5B). While our sampling was limited to fog events, the seasonal variability in bacterial occurrence suggests that wet conditions may enhance the occurrence of certain species. For example, *Serratia marcescens* occurred primarily during the early and late wet seasons, coinciding with higher fog frequency, while *Sphingomonas paucimobilis* was more common in drier periods. It must be noted that these findings are based on a limited dataset, and it remains possible that some species identified only in one season were present in others but at concentrations below the method detection threshold. More detailed statistical analyses and expanded sampling across seasons are required to confirm these trends and better understand the underlying mechanisms driving microbial distribution in fog water. In contrast to temperate forests, where fog often facilitates the dispersal of epiphytic microorganisms adapted to high humidity, or deserts, where fog sustains sparse microbial communities due to low nutrient availability, Amazonian fog may act as a dynamic vector for a diverse range of saprophytic and endophytic bacteria and fungi, potentially contributing to microbial colonization and nutrient cycling in tropical ecosystems.

Our findings revealed the presence of *Ralstonia pickettii*, a ubiquitous aerobic gram-negative, oxidase-positive, non-fermentative, rod-shaped bacterium, which has biodegradative abilities and thrives under low nutrient (oligotrophic) conditions[48]. *Serratia marcescens* is a gram-negative,

facultatively anaerobic bacterium that is differentiated from other gram-negative bacteria by its ability to perform casein hydrolysis, which allows it to produce extracellular metalloproteinases[49]. *Pseudomonas putida* has been documented to suggest potential for nutrient cycling, bioremediation, and plant growth promotion in soil and rhizosphere environments[51,52]. While these roles are plausible in the Amazonian fog context due to the presence of viable *Pseudomonas cells, further studies are needed to confirm their activity in fog droplets.* A study conducted by Dutra et al. (2023)[52] evaluated the efficiency of *Sphingomonas spp*. bacteria in phosphate solubilization and demonstrated that inoculation with these bacteria significantly increased the available phosphorus content in solution, thus highlighting their potential to enhance phosphorus availability for plants[53].

The recovered fungi from fog water samples from the Amazon rainforest showed high inter- and intraseasonal variability in isolated strains. Our study identified seven distinct fungal species in fog samples (Fig. 5B), with *Aspergillus niger* being most prevalent, occurring in 43% of fog samples, along with the closely related *Penicillium* species. These cosmopolitan fungi are found in both natural and anthropogenic environments[53]. They have been extensively studied, as they are producers of enzymes such as amylase, cellulase, pectinase, protease, and phytase[54]. *Aspergillus*, a primary organic matter decomposer, is more prevalent in warmer climates. *Sterile mycelia,* fungi without known sexual or asexual spores, represented 14% of the identified fungi, showcasing their notable presence. Additionally, *Rhodotorula mucilaginosa* and *Alternaria sp*. were present in 13% of the samples each (Fig. 5B). The transport of fungal spores plays a key role in shaping the spatial distribution and abundance of fungal communities in tropical ecosystems, which may suggest potential for organic matter decomposition and nutrient cycling. While these fungi are known to contribute to organic matter decomposition and nutrient cycling in other ecosystems[53,54], direct evidence of these functions in Amazonian fog droplets remains to be established through targeted functional studies.

Aspergillus and *Penicillium* spores had higher prevalence in fog samples collected during the late wet season, which featured more prolonged low-visibility fog events compared to the late dry season, potentially reflecting their moisture-driven growth and reproduction cycle. In contrast, others, including *Sphingomonas paucimobilis*, were more commonly observed during drier conditions. The fact that these species could be isolated from fog water samples suggests that fog could

facilitate the dispersal and deposition of specific fungal taxa, potentially influencing microbial colonization patterns across the rainforest. Notably, the fungal species identified in fog water were also previously observed in dry air above the canopy[28], supporting the inference of a local source from within or below the canopy.

Although culture-based methods identified specific microbial species with known ecological roles, it is critical to recognize that only a small fraction of environmental microorganisms are cultivable using standard laboratory techniques. Historical estimates suggest that less than 1% of bacterial species are cultivable[54], though recent advances indicate this proportion may be higher in certain environments, with up to 34.9% of bacterial taxa having culturable relatives[55]. In this study, flow cytometry detected significantly higher concentrations of viable microbial cells compared to the culturable species identified, suggesting that the total microbial diversity in Amazonian fog is substantially greater than that captured by culturing. This underscores the importance of combining culture-based and non-culture-based approaches to comprehensively characterize fog microbial communities and highlights the need for future studies using metagenomic techniques to fully elucidate the diversity and functional roles of non-culturable microorganisms.

It is important to note, however, that the culture medium used (Dichloran Rose Bengal) in the current study may have selectively favored certain species over others, representing a potential limitation of this study. Specifically, DRBC may underestimate fungal diversity by 20–30% compared to non-selective media, as it favors slow-growing, xerotolerant fungi like *Aspergillus* and *Penicillium*[56]. To overcome the limitations of the DRBC culture medium in capturing the full spectrum of fungal diversity, future studies could employ metagenomic approaches to provide a more comprehensive analysis of microbial communities in Amazonian fog droplets. To address concerns about potential contamination, we implemented rigorous protocols as follows. All of the fungal types observed in our Amazon fog samples mostly release asexual conidia, 3 to 10 µm in diameter, into the atmosphere, along with associated hyphal fragments and volatile organic compounds. Since all the fungal spores identified here were asexual, they do not have an associated release of propulsion fluids that are known for their CCN activity. Fog-mediated deposition of viable microbes may suggest a potential for promoting microbial colonization and decomposition of organic matter, thereby possibly contributing to nutrient cycling in rainforest ecosystems[31,56].

While our culture-dependent approach reveals seasonal patterns in culturable taxa (e.g., higher prevalence of *Sphingomonas* in wet season samples), these observations are subject to culturing biases and drawbacks in data analysis and do not capture the full microbial diversity. Future studies integrating metagenomics could complement these findings to assess the genetic material of living and dead organisms, as well as unculturable fractions.

To better understand the potential ecological roles of the isolated organisms and put them in a wider context, we tried to compare microbial communities in fog with those in background aerosols. However, due to methodological differences (selective culturing vs. metabardocing), comparisons are challenging and must be interpreted with caution. For instance, Souza et al. (2021) used metabarcoding at the ATTO site to show that below canopy aerosol communities are dominated by *Proteobacteria*, *Firmicutes*, and *Actinobacteria*, with seasonal compositional shifts driven by humidity, temperature, and potential changes in sources. Given differences in taxonomic resolution, we compared only on family level, finding that bacterial families of our isolates comprise ~31 % of the community found by Souza et al. (2021) across seasons, with only *Comamonadaceae* (*Delftia acidovorans*) and *Ralstoniaceae* (*Ralstonia pickettii*) being absent. The overlap suggests common sources and selective recruitment of FCN from the broader bioaerosol community.

In the current study, most fungi isolated from fog water belong to *Ascomycota,* with *Penicillium* being prevalent and *Cladosporium* occurring at low frequency in fog. In contrast to that, Mota de Oliveira et al. (2022)[64] reported 30% basidiospores among airborne fungal OTUs at 300 m and Weber et al. (in prep.) found a dominance of *Basidiomycota* at 42 m during the wet season. In the latter study, only 7.3 % of the observed genera belonged to Ascomycota, with only *Penicillium* and *Cladosporium* occurring daily. The frequent occurrence of *Penicillium* both in bioaerosol and in fog may suggest it to act as FCN. This interpretation has to be taken with caution, as the chosen culture medium favors molds and may underrepresent Basidiomycota. These differences between studies may highlight fog's modulation of bioaerosol dynamics, calling for an integrated sampling of bioaerosol and fog to clarify the impact of fog on microbial dispersion and activity.

Climate Change Implications

As outlined in the Introduction, the Amazon rainforest is critical to global climate and hydrological cycles. However, climate change and deforestation are projected to reduce atmospheric moisture and extend the late dry seasons, limiting the supersaturation conditions necessary for fog formation[57,58]. Increased biomass burning elevates aerosol concentrations (up to 10^4 cm^{-3}), including black carbon, which warms the boundary layer and suppresses fog development[16]. Concurrently, deforestation reduces primary biological aerosol particles (PBAPs), key FCN, further constraining fog formation[21,59]. These changes may disrupt fog-mediated processes outlined in Results, such as microbial dispersal, impacting biodiversity and biogeochemical cycles in forest–savanna transition zones. Such disruptions could potentially affect interactions, such as *Pseudomonas*-mediated phosphorus mobilization from Saharan dust, which might compromise ecosystem fertility under warmer, drier conditions. The direct response of fog to multiple drivers remains poorly understood due to the scarcity of long-term, high-resolution fog observations; however, most models and studies consistently predict a decline in fog frequency under warmer, drier, and more polluted conditions[60,61]. While this study demonstrates the presence of viable microbes in fog droplets, further research is needed to confirm fog's specific role in microbial dispersal compared to other atmospheric mechanisms and its direct contribution to ecosystem processes. Notably, *Pseudomonas* also plays a crucial role in mobilizing phosphorus from Saharan dust that is annually deposited in the Amazon, thereby enhancing soil fertility and supporting forest productivity. The interaction between fog-transported microorganisms and Saharan dust deposited in the Amazon may represent a key biogeochemical process. For instance, *Pseudomonas spp*. can colonize dust particles and enhance phosphorus solubilization by up to 30% in tropical soils[62]. By facilitating the deposition of these microorganisms onto foliar surfaces and soil, fog may amplify nutrient mobilization from external sources, such as transcontinental dust. Changes in fog frequency, potentially driven by climate change, could disrupt this interaction, with possible implications for the fertility of the Amazonian ecosystem. While visibility data from 2014 to 2023 at ATTO (Fig. 2) indicate seasonal variability in fog, long-term trends remain unclear, highlighting the need for further monitoring.

Conclusion

This study presents a first investigation and taxonomic characterization of viable microbial communities within Amazonian fog droplets, using flow cytometry for quantification and culture based MALDI-TOF for identification. The detection of metabolically active bacterial and fungal taxa, such as *Serratia marcescens*, *Ralstonia pickettii*, *Sphingomonas paucimobilis*, and *Aspergillus niger*, suggests that fog may have the potential to serve as a viable habitat and redistribute ecologically relevant microorganisms across the rainforest canopy. By facilitating the vertical transport and deposition of viable microbes, fog serves as an important component of Amazonian ecosystem dynamics, with observed intra- and interseasonal variability in cell numbers potentially reflecting meteorological influences and background aerosol properties. Climate-driven shifts in fog frequency and structure may alter microbial dispersal and deposition dynamics, with potential downstream effects on tropical ecosystem functioning. These findings highlight fog as a dynamic interface linking microbial processes in the forest canopy with broader atmospheric and ecological systems. By documenting viable microbial content in Amazonian fog, this study establishes a foundation for future investigations into the role of fog in tropical bioaerosol dynamics and its implications for ecosystem resilience under changing environmental conditions.

References

1. Lovejoy, T. E. & Nobre, C. Amazon Tipping Point. *Sci. Adv.* **4** (2):eaat2340, (2018).
2. Boulton, C. A., Lenton, T. M. & Boers, N. Pronounced loss of Amazon rainforest resilience since the early 2000s. *Nat. Clim. Change* **12**, 271–278 (2022).
3. Gatti, L. V. et al. Increased Amazon carbon emissions mainly from decline in law enforcement. Nature **621**, 318–323 (2023). https://doi.org/10.1038/s41586-023-06390-0.
4. Albert, J. S. et al. Human impacts outpace natural processes in the Amazon. *Science* **379**, eabo5003 (2023).
5. Flores, B. M. et al. Critical transitions in the Amazon forest system. *Nature* **626**, 555–564 (2024).
6. Artaxo, P. et al. Tropical and Boreal Forest – Atmosphere Interactions: A review. *Tellus B* **74(1)**, 24 (2022).
7. Staal, A. et al. Feedback between drought and deforestation in the Amazon. *Environ. Res. Lett.* **15**, 044024 (2020).
8. Esquivel-Muelbert, A. et al. Compositional response of Amazon forests to climate change. *Glob. Change Biol.* **25**, 39–56 (2019).
9. Pearce, F. Weather makers. *Science* **368**, 1302–1305 (2020).
10. Koračin, D. et al. Marine fog: A review. *Atmos. Res.* **143**, 142–175 (2014).

11. Barnes, G. & Gentle, I. Interfacial Science: An Introduction. (Oxford Univ. Press USA, 2011), pp30-34.
12. Petters, M. D. & Kreidenweis, S. M. A single parameter representation of hygroscopic growth and cloud condensation nucleus activity. *Atmos. Chem. Phys.* **7**, 1961–1971 (2007).
13. Zhang, G. et al. Fog/cloud processing of atmospheric aerosols from a single particle perspective: A review of field observations. *Atmos. Environ.* **329**, 120536 (2024).
14. Lakra, K. & Avishek, K. A review on factors influencing fog formation, classification, forecasting, detection and impacts. *Rend. Lincei. Sci. Fis. Nat.* **33**, 319–353 (2022).
15. Anber, U., Gentine, P., Wang, S. & Sobel, A. H. Fog and rain in the Amazon. *Proc. Natl. Acad. Sci. U.S.A.* **112**, 11473–11477 (2015).
16. Wainwright, C., Chang, R. Y.-w. & Richter, D. Aerosol activation in radiation fog at the Atmospheric Radiation Program Southern Great Plains site. *J. Geophys. Res. Atmos.* **126**, e2021JD035358 (2021).
17. Pöhlker, M. L. et al. Long-term observations of cloud condensation nuclei over the Amazon rain forest – Part 2: Variability and characteristics of biomass burning, long-range transport, and pristine rain forest aerosols. *Atmos. Chem. Phys.* **18**, 10289–10331 (2018).
18. Pöhlker, M. L. et al. Long-term observations of cloud condensation nuclei in the Amazon rain forest – Part 1: Aerosol size distribution, hygroscopicity, and new model parametrizations for CCN prediction. *Atmos. Chem. Phys.***16**, 15709–15740 (2016).
19. Noone, K. J. et al. Changes in aerosol size- and phase distributions due to physical and chemical processes in fog. *Tellus B* **44**, 489-504 (1992).
20. Motos, G. et al. Droplet activation behaviour of atmospheric black carbon particles in fog as a function of their size and mixing state. *Atmos. Chem. Phys.* **19**, 2183–2207 (2019).
21. Singh, V. P., Gupta, T., Tripathi, S. N., Jariwala, C. & Das, U. Experimental study of the effects of environmental and fog condensation nuclei parameters on the rate of fog formation and dissipation using a new laboratory scale fog generation facility. *Aerosol Air Qual. Res.* **11**, 140–154 (2011).
22. Huffman, J. A. et al. High concentrations of biological aerosol particles and ice nuclei during and after rain. *Atmos. Chem. Phys.* **13**, 6151–6164 (2013).
23. Zhao, B. et al. Formation process of particles and cloud condensation nuclei over the Amazon rainforest: The role of local and remote new-particle formation. *Geophys. Res. Lett.* **49**, e2022GL100940 (2022).
24. Brito, J. et al. Ground-based aerosol characterization during the South American Biomass Burning Analysis (SAMBBA) field experiment. *Atmos. Chem. Phys.* **14**, 12069–12083 (2014).
25. Moran-Zuloaga, D. et al. Long-term study on coarse mode aerosols in the Amazon rain forest with the frequent intrusion of Saharan dust plumes. *Atmos. Chem. Phys.* **18**, 10055–10088 (2018).
26. Pöhlker, C. et al. Biogenic potassium salt particles as seeds for secondary organic aerosol in the Amazon. *Science.* **337**, 1075–1078 (2012).
27. China, S. et al. Fungal spores as a source of sodium salt particles in the Amazon basin. *Nat. Commun.* **9**, 4793 (2018).
28. Barbosa, C. G. G. et al. Identification and quantification of giant bioaerosol particles over the Amazon rainforest. *NPJ Clim. Atmos. Sci.* **5**, 73 (2022).
29. Tortosa, G. et al. Involvement of the metabolically active bacteria in the organic matter degradation during olive mill waste composting. *Sci. Total Environ.* **789**, 147975 (2021).
30. Evans, S. E., Dueker, M. E., Logan, J. R. & Weathers, K. C. The biology of fog: results from coastal Maine and Namib Desert reveal common drivers of fog microbial composition. *Sci. Total Environ.* **647**, 1547–1556 (2019).

31. Gao, Y. et al. Bacterial spore germination receptors are nutrient-gated ion channels. *Science* **380**, 387–391 (2023).
32. Charpentier, T. et al. Culturable bacteria in clouds at Réunion, tropical island. *Aerobiologia* **40**, 297–302 (2024).
33. Andreae, M. O. et al. The Amazon Tall Tower Observatory (ATTO): overview of pilot measurements on ecosystem ecology, meteorology, trace gases, and aerosols. *Atmos. Chem. Phys.* **15**, 10723–10776 (2015).
34. Brill, S. et al. Automated atmospheric profiling with the Robotic Lift (ROLI) at the Amazon Tall Tower Observatory. *EGU* (2025) doi:10.5194/egusphere-2025-295.
35. Chazotte, B. Labeling Nuclear DNA with Hoechst 33342. *Cold Spring Harb. Protoc.* **2011**, pdb.prot5557 (2011).
36. De Matos Castro E Silva, D. et al. A new culture medium for recovering the agents of Cryptococcosis from environmental sources. *Braz. J. Microbiol.* **46**, 355–358 (2015).
37. Mantoani, M. C. et al. Rainfall effects on vertical profiles of airborne fungi over a mixed land-use context at the Brazilian Atlantic Forest biodiversity hotspot. *Agric. For. Meteorol.* **331**, 109352 (2023).
38. Bizzini, A. & Greub, G. Matrix-assisted laser desorption ionization time-of-flight mass spectrometry, a revolution in clinical microbial identification. *Clin. Microbiol. Infect.* **16**, 1614–1619 (2010).
39. Mantoani, M. C. et al. Biological characterisation of hailstones from two storms in South Brazil. *Aerobiologia* **1**, 98–108 (2024).
40. Yáñez-Serrano, A. M. et al. Diel and seasonal changes of biogenic volatile organic compounds within and above an Amazonian rainforest. *Atmos. Chem. Phys.* **15**, 3359–3378 (2015).
41. Hammer, E. et al. Size-dependent particle activation properties in fog during the ParisFog 2012/13 field campaign. *Atmos. Chem. Phys.* **14**, 10517–10533 (2014).
42. Prass, M. et al. Bioaerosols in the Amazon rain forest: temporal variations and vertical profiles of Eukarya, Bacteria, and Archaea. *Biogeosciences* **18**, 4873–4887 (2021).
43. Amato, P. et al. Survival and ice nucleation activity of bacteria as aerosols in a cloud simulation chamber. *Atmos. Chem. Phys*. **15**, 6455–6465 (2015).
44. Pouzet, G. et al. Atmospheric processing and variability of biological ice nucleating particles in precipitation at OPme, France. *Atmosphere* **8**, 229 (2017).
45. Péguilhan, R., Rossi, F., Rué, O., Joly, M. & Amato, P. Comparative analysis of bacterial diversity in clouds and aerosols. *Atmos. Environ.* **298**, 119635 (2023).
46. Ryan, M. P. & Adley, C. C. Ralstonia spp.: emerging global opportunistic pathogens. *Eur. J. Clin. Microbiol. Infect. Dis.* **33**, 291–304 (2014).
47. White, D. C., Sutton, S. D. & Ringelberg, D. B. The genus Sphingomonas: physiology and ecology. *Curr. Opin. Biotechnol.* **7**, 301–306 (1996).
48. Ryan, M. P., Pembroke, J. T. & Adley, C. C. *Ralstonia pickettii* in environmental biotechnology: potential and applications. *J. Appl. Microbiol.* **103**, 754–764 (2007).
49. Hejazi, A. & Falkiner, F. R. *Serratia marcescens*. *J. Med. Microbiol.* **46**, 903–912 (1997).
50. Yousuf, J. et al. Nitrogen fixing potential of various heterotrophic Bacillus strains from a tropical estuary and adjacent coastal regions. *J. Basic Microbiol.* **57**, 922–932 (2017).
51. Loeschcke, A. & Thies, S. *Pseudomonas putida*—a versatile host for the production of natural products. *Appl. Microbiol. Biotechnol.* **99**, 6197–6214 (2015).
52. Dutra, M. P., Baldotto, M. A., Da Silva, L. F., Baldotto, L. E. B. & De Oliveira, V. C. Bacterias solubilizadoras de fosfato em associação com termofosfato e fertilizante organomineral. (2023). doi:10.22533/at.ed.1632329114. pp. 37–51.

53. Narayanan, M. et al. Water hyacinth biochar and *Aspergillus niger* biomass amalgamation potential in removal of pollutants from polluted lake water. *J. Environ. Chem. Eng.* **9**, 105574 (2021).
54. Amann, R. I., Ludwig, W. & Schleifer, K.-H. Phylogenetic identification and in situ detection of individual microbial cells without cultivation. Microbiol. Rev. 59, 143–169 (1995)
55. Martiny, A. C. High proportions of bacteria are culturable across major biomes. ISME J. 13, 2125–2128 (2019).
56. Maia, T. F. & Fraga, M. E. Bioprospecting Aspergillus section Nigri in Atlantic Forest soil and plant litter. *Arq. Inst. Biol.* **84**, e0502015 (2017).
57. Marengo, J. A. et al. Changes in climate and land use over the Amazon region: current and future variability and trends. *Front. Earth Sci.* **6**, 228 (2018).
58. Spracklen, D. V. & Garcia-Carreras, L. The impact of Amazonian deforestation on Amazon basin rainfall. *Geophys. Res. Lett.* **42**, 9546–9552 (2015).
59. Gatti, L. V. et al. Amazonia as a carbon source linked to deforestation and climate change. *Nature* **595**, 388–393 (2021).
60. Vautard, R., Yiou, P. & Van Oldenborgh, G. J. Decline of fog, mist and haze in Europe over the past 30 years. *Nat. Geosci.* **2**, 115–119 (2009).
61. Gultepe, I. et al. FOG research: A review of past achievements and future perspectives. *Pure Appl. Geophys.* **164**, 1121–1159 (2007).
62. Panhwar, Q. A. et al. Biochemical and molecular characterization of potential phosphate-solubilizing bacteria in acid sulfate soils and their beneficial effects on rice growth. *PLoS* ONE 9, e97241 (2014).
63. Souza, F. F. C. et al. Influence of seasonality on the aerosol microbiome of the Amazon rainforest. Science of the Total Environment 754, 144092 (2021).
64. Mota de Oliveira, S. et al. Life is in the air: An expedition into the Amazonian atmosphere. Frontiers in Ecology and Evolution 10, 789791 (2022).

Acknowledgments

The authors gratefully acknowledge the essential financial support that made this research possible. We thank ATTO and FINEP (Financing Agency for Studies and Projects) for funding Project 01.22.0258.01, which provided the necessary infrastructure and resources for the development of this work. We also express our gratitude to the National Council for Scientific and Technological Development (CNPq) for supporting the National Institute of Science and Technology (INCT) through grant 408944/2024-2. Special thanks are extended to Bruna Sebben for the master's scholarship awarded by CAPES (Coordination for the Improvement of Higher Education Personnel), and to Emerson Hara for the postdoctoral fellowship funded by CNPq. These scholarships enabled full dedication to the research activities presented in this study. This research used resources at the Environmental Molecular Sciences Laboratory (EMSL), a DOE Office of Science User Facility. EMSL is sponsored by the Biological and Environmental Research program and operated under Contract No. DE-AC05-76RL01830. Without the generous support of these institutions and agencies, and the commitment of the scholarship recipients, this work would not have been feasible.

Author contributions

Ricardo H. M. Godoi led the project conceptualization, supervised the study, contributed to formal analysis, investigation, data curation, visualization, writing – original draft, writing – review & editing, and funding acquisition. Meinrat O. Andreae contributed to project conceptualization, investigation, data curation, writing – original draft, review & editing, and funding acquisition. Ulrich Pöschl contributed to conceptualization, formal analysis, writing – original draft, review & editing, and funding acquisition. Scot T. Martin contributed to conceptualization, formal analysis, writing – original draft, review & editing, and funding acquisition. Christopher Pöhlker contributed to conceptualization, formal analysis, resources, writing – original draft, review & editing, and funding acquisition. Bettina Weber contributed to conceptualization, software development, resources, writing – original draft, review & editing, and funding acquisition. Sanja Potgieter-Vermaak contributed to formal analysis, data curation, writing – original draft, and review & editing. Emerson L. Y. Hara contributed to methodology, validation, formal analysis, investigation, writing – original draft, and visualization. Bruna G. Sebben contributed to methodology, software, validation, formal analysis, investigation, data curation, writing – original draft, review & editing, and visualization. Philip E. Taylor contributed to conceptualization, formal analysis, investigation, writing – original draft, and review & editing. Dulcilena M. Castro e Silva contributed to validation, formal analysis, investigation, resources, data curation, and writing – original draft. Sebastian Brill contributed to validation, software, formal analysis, investigation, resources, data curation, writing – original draft, review & editing, and visualization. Valter B. Duo Filho contributed to validation, formal analysis, investigation, resources, and data curation. Glaucio Valdameri contributed to validation, formal analysis, investigation, resources, data curation, writing – original draft, and review & editing. Luciano F. Huergo contributed to methodology, formal analysis, data curation, writing – original draft, and review & editing. Rosaria R. Ferreira contributed to software, investigation, resources, and data curation. Cléo Q. Dias-Junior contributed to software, formal analysis, investigation, resources, data curation, writing – original draft, and review & editing. Maurício C. Mantoani contributed to methodology, validation, formal analysis, and visualization. Fábio L. T. Gonçalves contributed to formal analysis, resources, writing – original draft, and review & editing. Rachel I. Albrecht contributed to software, formal analysis, writing – original draft, and review & editing. Nurun N. Lata contributed to validation, formal analysis, investigation, resources, and data curation. Gregory Vandergrift contributed to validation, formal analysis, investigation, and data curation. Swarup China contributed to formal analysis, resources, writing – original draft, review & editing, and funding acquisition. Carlos I. Yamamoto contributed to validation, formal analysis, resources, data curation, writing – original draft, and review & editing. Rodrigo F. C. Marques contributed to formal analysis, resources, writing – original draft, and review & editing. Rodolfo D. Piazza contributed to validation, formal analysis, investigation, resources, data curation, and writing – original draft. Rodrigo A. F. Souza contributed to formal analysis, investigation, resources, data curation, writing – original draft, and review & editing. Theotonio Pauliquevis contributed to validation, formal analysis, investigation, data curation, writing – original draft, and review & editing. Paulo Artaxo contributed to

conceptualization, formal analysis, writing – original draft, and review & editing. Luiz A. T. Machado contributed to software, formal analysis, data curation, writing – original draft, and review & editing. Heitor Evangelista contributed to formal analysis, data curation, writing – original draft, and review & editing. Jéssica C. Santos-Silva contributed to validation, formal analysis, investigation, data curation, writing – original draft, and visualization. Subha S. Raj contributed to formal analysis, investigation, resources, data curation, writing – original draft, and visualization. Jens Weber contributed to validation, formal analysis, investigation, resources, writing – original draft, review & editing, and visualization. Laudemir C. Varanda contributed to validation, formal analysis, data curation, writing – original draft, and review & editing. Ivan Kourtchev contributed to formal analysis, data curation, writing – original draft, and review & editing.

Competing interests

The authors declare no competing interests.

Supplementary information

The online version contains supplementary material available

Data availability

The datasets generated during and/or analysed during the current study are available in the Zenodo repository at https://doi.org/10.5281/zenodo.18255540. The SMPS data used in this analysis were obtained from the associated publication and are available at https://doi.org/10.1038/s41561-024-01585-0. All other data supporting the findings of this study are available within the article and its Supplementary Information files, including Source Data.

FIGURE LEGENDS

Fig. 1 Diurnal pattern of visibility at ATTO, depicted by month. Visibility data from Sep 2014 until Jan 2023 has been averaged here. The visibility trend shows a clear reduction during early morning hours, typically reaching a minimum around 04:00 local time (LT), followed by a sudden increase in visibility with the onset of solar heating between 06:00 and 07:00. A secondary dip in visibility

occurs in the late afternoon, coinciding with typical rain shower occurrences during this time. Each colored line represents the average visibility for a different month, with the legend indicating the respective months from January (01) to December (12).

Fig. 2 Monthly variation in atmospheric visibility at the Amazon Tall Tower Observatory (ATTO). Visibility measurements during fog events, excluding rainfall periods (±7 hours). Diamonds represent median visibility values.

Fig. 3 A-B Time series of precipitation (*P*), relative humidity (RH %), visibility (Vis) and aerosol abundance for fog sampling periods 1 (April 25 to May 9, 2022) and 2 (October 13 to October 2022) of the present study. The middle panel shows a contour plot of the aerosol surface size distribution (d*S*/dlog*D*) for the size range from 300 nm to 10 µm. The bottom panel shows a contour plot of the aerosol number size distribution (d*N*/dlog*D*) for the size range from 10 nm to 400 nm. Green boxes indicate the fog sampling periods analyzed in this study. For sample S3, minimal precipitation (P < 0.5 mm/h) occurred intermittently but did not compromise fog dominance.

Fig. 4. Vertical profiles between 14 January and 16 January 2023 at ATTO, covering the analyzed fog event S11 on 15 January 2023. (A) Precipitation (mm) and temperature (°C) measured at 325 m. (B–H) Vertical profiles from 8–318 m of (B) temperature (°C), (C) relative humidity (%), (D) specific humidity (g kg^{-1}), (E) visibility (m), (F) aerosol number concentration between 300 nm and 10 µm (cm^{-3}), (G) horizontal wind speed (m s^{-1}), and (H) wind direction (degrees), measured by the Robotic Lift (RoLi), an automated profiling platform at the 325 m tower. Date and time are shown in local time (UTC–4). Shaded areas in panel A indicate nighttime periods.

Fig. 5 Microbial cell abundance and culturable taxa in Amazonian fog. (A) Total microbial cell counts (103 per ml of fog water) determined by flow cytometry for 13 fog samples collected at the Amazon Tall Tower Observatory (ATTO) during three seasonal campaigns: late wet season (purple), late dry season (yellow), and early wet season (blue). Seasonal colors correspond to sampling campaigns. (B) Occurrence of culturable bacterial (left) and fungal (right) taxa identified in each sample. Filled circles represent the presence of each taxon, with circle size proportional to the number of observations per sample. Bar lengths indicate the overall frequency of each taxon: black for bacteria, grey for fungi. The overall frequency of each taxon was calculated as the percentage of samples in which the taxon was detected (number of samples with the taxon present divided by the total number of samples, 13. Taxa were identified by cultivation and MALDI-TOF MS. See Methods for details.

Campaign	Sample	Date	Sampling time (h)	pH	Zeta Potential (mV)
Campaign 1	S1	04/26/2022	2am-7am	5.96	-16.2 ± 2.2
	S2	04/30/2022	2am-7am	6.15	-5.87 ± 1.9
	S3	5/1/2022	5pm-7am	5.77	-14.3 ± 1.0
	S4	5/4/2022	8pm-9am	5.57	-11.9 ± 1.9
	S5	5/6/2022	5pm-9am	5.70	-10.3 ± 1.6
	S6	5/7/2022	5pm-9am	5.26	-16.1 ± 0.6
Campaign 2	S7	10/13/2022	10pm-8am	5.85	-9.8 ± 4.3
	S8	10/15/2022	10pm-8am	5.24	-15.6 ± 0.8
	S9	10/17/2022	10pm-8am	4.98	-14.9 ± 1.1
	S10	10/19/2022	10pm-8am	5.26	-13.1 ± 2.6
Campaign 3	S11	01/14/2023	10pm-8am	7.31	-4.71 ± 1.1
	S12	01/17/2023	10pm-8am	7.50	-10.8 ± 1.5
	S13	01/20/2023	10pm-8am	6.76	-7.3 ± 1.7

Editorial summary:
Amazonian fog samples contain viable microbes, suggesting fog plays a role microbial dispersal, colonization and nutrient cycling, according to analyses of fog samples from a tall tower observatory.

Peer review information:
Communications Earth & Environment thanks the anonymous reviewers for their contribution to the peer review of this work. Primary Handling Editors: Yinon Rudich and Alice Drinkwater. A peer review file is available

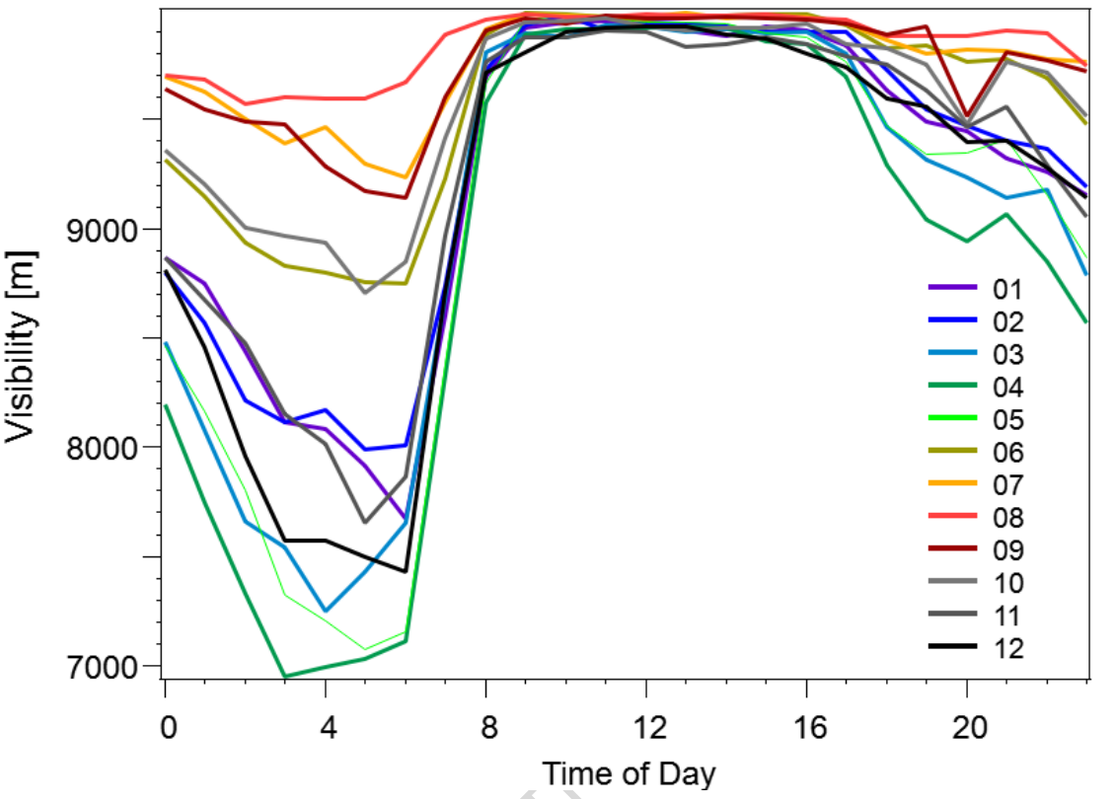

Fig. 2 Diurnal pattern of visibility at ATTO, depicted by month. Visibility data from Sep 2014 until Jan 2023 has been averaged here. The visibility trend shows a clear reduction during early morning hours, typically reaching a minimum around 04:00 local time (LT), followed by a sudden increase in visibility with the onset of solar heating between 06:00 and 07:00. A secondary dip in visibility occurs in the late afternoon, coinciding with typical rain shower occurrences during this time. Each colored line represents the average visibility for a different month, with the legend indicating the respective months from January (01) to December (12).

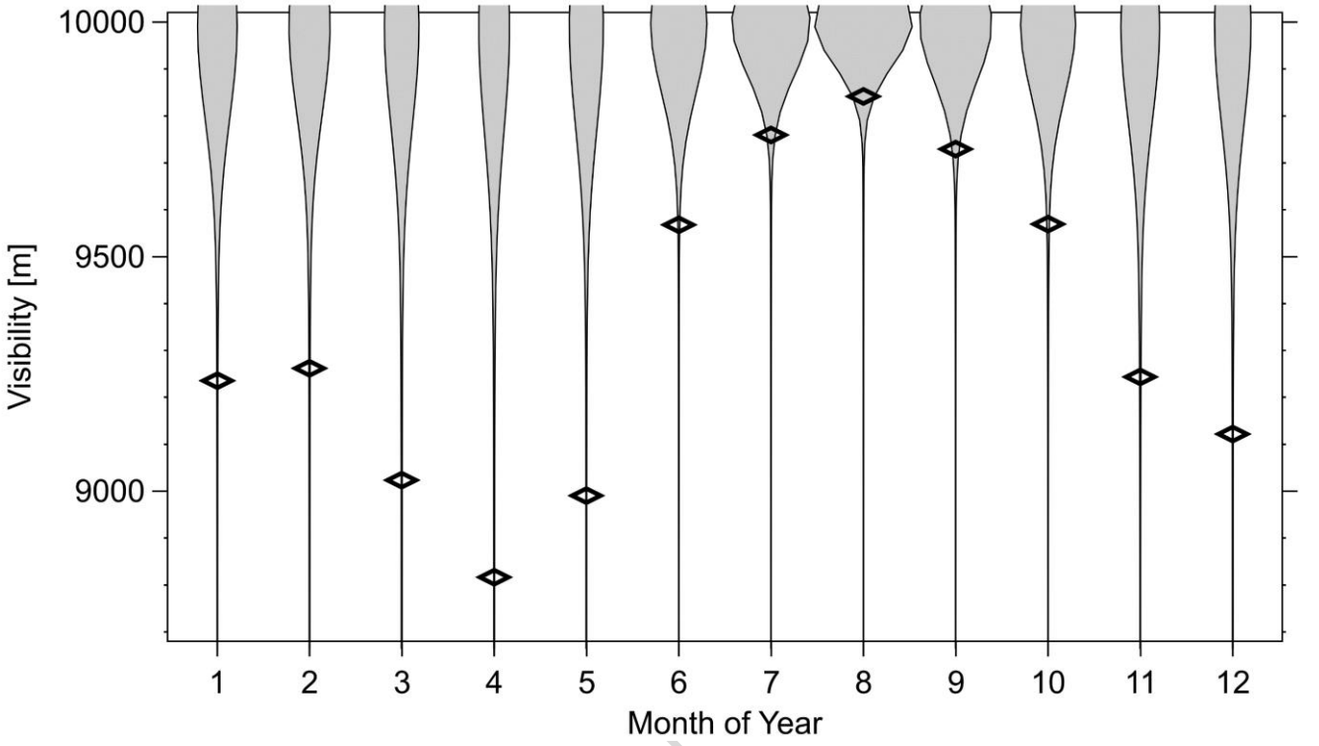

Fig. 2 Monthly variation in atmospheric visibility at the Amazon Tall Tower Observatory (ATTO). Visibility measurements during fog events, excluding rainfall periods (±7 hours). Diamonds represent median visibility values.

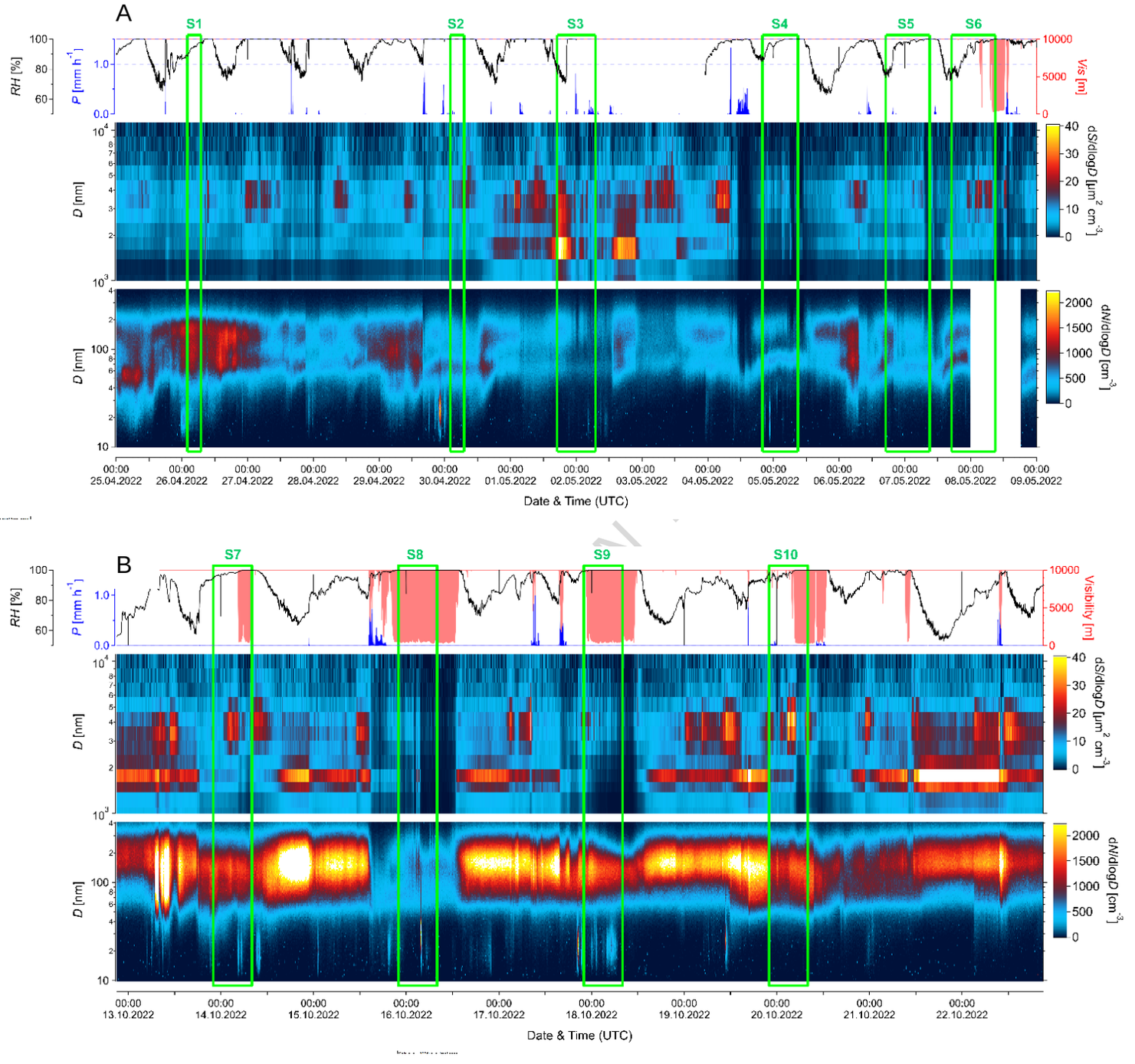

Fig. 3 A-B Time series of precipitation (*P*), relative humidity (RH %), visibility (Vis) and aerosol abundance for fog sampling periods 1 (April 25 to May 9, 2022) and 2 (October 13 to October 2022) of the present study. The middle panel shows a contour plot of the aerosol surface size distribution (d*S*/dlog*D*) for the size range from 300 nm to 10 µm. The bottom panel shows a contour plot of the aerosol number size distribution (d*N*/dlog*D*) for the size range from 10 nm to 400 nm. Green boxes indicate the fog sampling periods analyzed in this study. For sample S3,

minimal precipitation (P < 0.5 mm/h) occurred intermittently but did not compromise fog dominance.

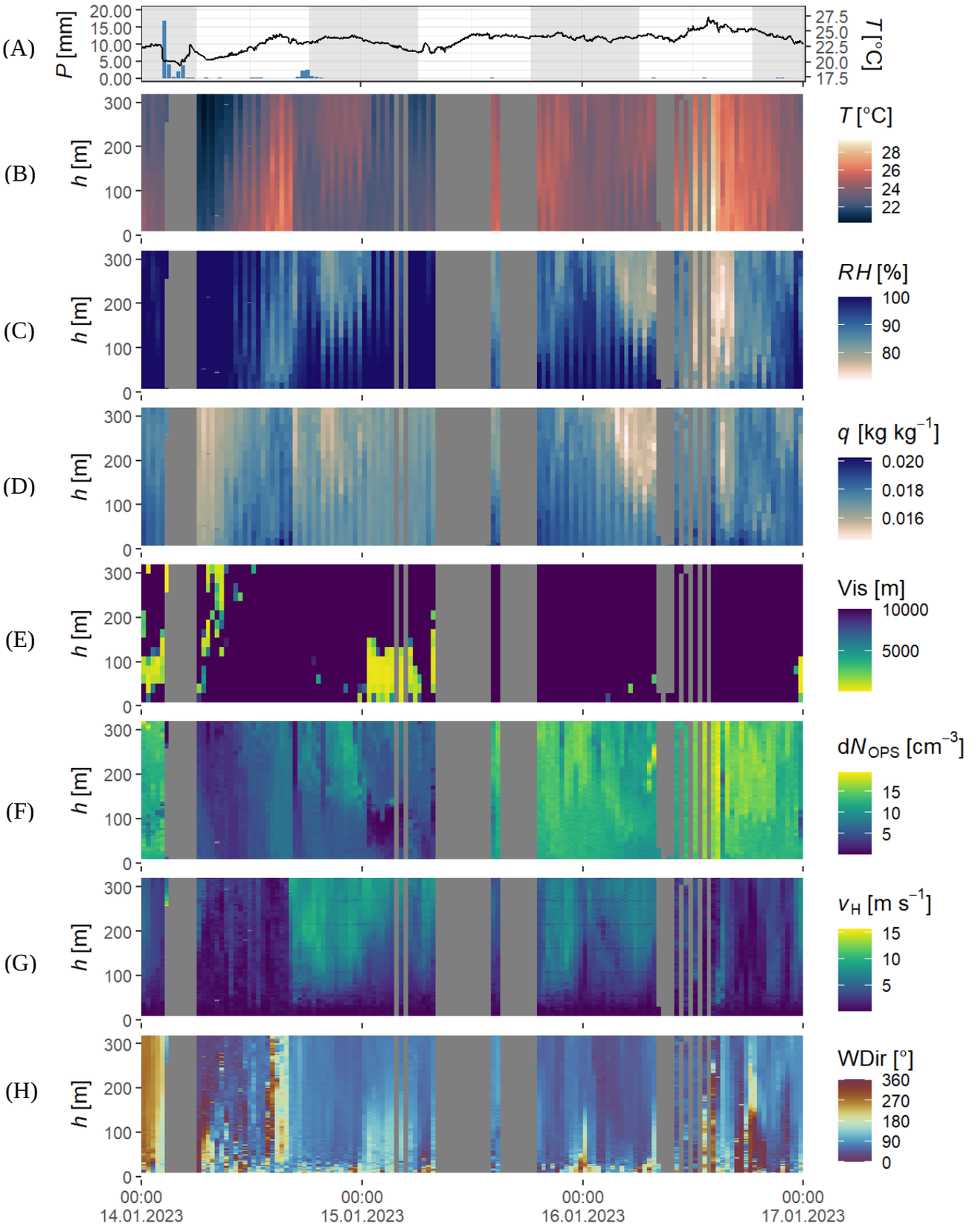
(A)
P [mm]
20.00
15.00
10.00
5.00
0.00
T [°C]
27.5
25.0
22.5
20.0
17.5
(B)
h [m]
300
200
100
0
T [°C]
28
26
24
22
(C)
RH [%]
100
90
80
(D)
q [kg kg−1]
0.020
0.018
0.016
(E)
Vis [m]
10000
5000
(F)
dNOPS [cm−3]
15
10
5
(G)
vH [m s−1]
15
10
5
(H)
WDir [°]
360
270
180
90
0
00:00
14.01.2023
00:00
15.01.2023
00:00
16.01.2023
00:00
17.01.2023

Fig. 4. Vertical profiles between 14 January and 16 January 2023 at ATTO, covering the analyzed fog event S11 on 15 January 2023. (A) Precipitation (mm) and temperature (°C) measured at 325 m. (B–H) Vertical profiles from 8–318 m of (B) temperature (°C), (C) relative humidity (%), (D) specific humidity (g kg^{-1}), (E) visibility (m), (F) aerosol number concentration between 300 nm and 10 µm (cm^{-3}), (G) horizontal wind speed (m s^{-1}), and (H) wind direction (degrees), measured by the Robotic Lift (RoLi), an automated profiling platform at the 325 m tower. Date and time are shown in local time (UTC–4). Shaded areas in panel A indicate nighttime periods.

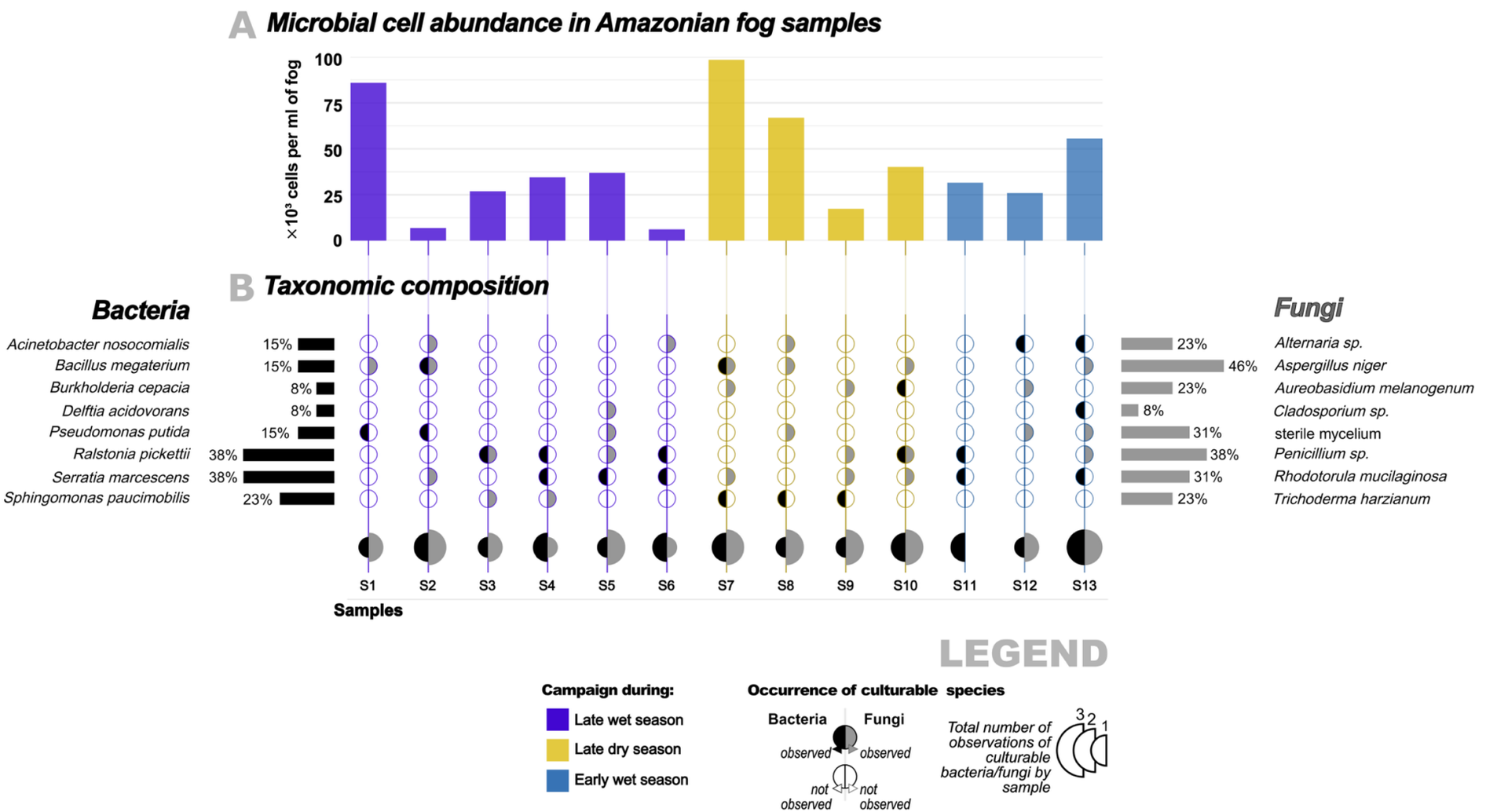
A Microbial cell abundance in Amazonian fog samples
×10³ cells per ml of fog
100
75
50
25
0
B Taxonomic composition
Bacteria
Acinetobacter nosocomialis
Bacillus megaterium
Burkholderia cepacia
Delftia acidovorans
Pseudomonas putida
Ralstonia pickettii
Serratia marcescens
Sphingomonas paucimobilis
15%
15%
8%
8%
15%
38%
38%
23%
Fungi
Alternaria sp.
Aspergillus niger
Aureobasidium melanogenum
Cladosporium sp.
sterile mycelium
Penicillium sp.
Rhodotorula mucilaginosa
Trichoderma harzianum
23%
46%
23%
8%
31%
38%
31%
23%
S1
S2
S3
S4
S5
S6
S7
S8
S9
S10
S11
S12
S13
Samples
LEGEND
Campaign during:
Late wet season
Late dry season
Early wet season
Occurrence of culturable species
Bacteria
Fungi
observed
observed
not observed
not observed
Total number of observations of culturable bacteria/fungi by sample
3
2
1

Fig. 5 Microbial cell abundance and culturable taxa in Amazonian fog. (A) Total microbial cell counts (10^3 per ml of fog water) determined by flow cytometry for 13 fog samples collected at the Amazon Tall Tower Observatory (ATTO) during three seasonal campaigns: late wet season (purple), late dry season (yellow), and early wet season (blue). Seasonal colors correspond to sampling campaigns. (B) Occurrence of culturable bacterial (left) and fungal (right) taxa identified in each sample. Filled circles represent the presence of each taxon, with circle size proportional to the number of observations per sample. Bar lengths indicate the overall frequency of each taxon: black for bacteria, grey for fungi. The overall frequency of each taxon was calculated as the percentage of samples in which the taxon was detected (number of samples with the taxon present divided by the total number of samples, 13. Taxa were identified by cultivation and MALDI-TOF MS. See Methods for details.